LASER & PHOTONICS REVIEWS

Laser Photonics Rev. **8,** No. 6, L93–L97 (2014) / **DOI** 10.1002/lpor.201400113

Abstract Grating couplers are key elements enabling the coupling of light between planar waveguide circuits and optical fibers. In this work, it is demonstrated using simulations and experiments that a high coupling efficiency can be achieved for an arbitrary buried oxide thickness by judicious adjustment of the grating radiation angle. The coupler strength is engineered by subwavelength structure, allowing straightforward apodization and single etch step fabrication. The design has been implemented using Fourier-eigenmode expansion and finite difference time domain methods. The measured coupling loss of a continuously apodized grating is −2.16 dB with a 3 dB bandwidth of 64 nm, therefore opening promising prospects for low-cost and high-volume fabrication using 193 nm deep-ultraviolet lithography. It is also shown by simulations that a coupling loss as low as −0.42 dB is predicted for a modified coupler structure with bottom mirror.

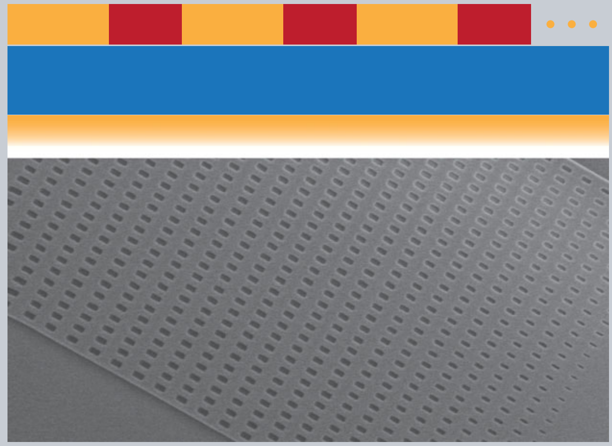

High-efficiency single etch step apodized surface grating coupler using subwavelength structure

Daniel Benedikovic[1,*], Pavel Cheben[2,*], Jens H. Schmid[2], Dan-Xia Xu[2], Jean Lapointe[2], Shurui Wang[2], Robert Halir[3], Alejandro Ortega-Moñux[3], Siegfried Janz[2], and Milan Dado[1]

1. Introduction

Silicon-on-insulator (SOI) is arguably the most promising platform for implementing complementary metal–oxide–semiconductor (CMOS)-compatible high-density planar waveguide photonic integrated circuits [1]. However, coupling between silicon waveguides of submicrometer cross-sections and optical fibers is inefficient due to largely disparate mode dimensions, which typically requires utilization of integrated mode size transformers [2]. Recent developments have shown that coupling efficiencies can be significantly improved by using fiber–chip edge couplers and surface grating couplers [3–18]. Edge coupling with inversely tapered waveguides shows high efficiencies and broadband operation [3–5]. A robust fabrication performance and minimal polarization dependence have been demonstrated for subwavelength grating (SWG) edge couplers [4]. However, edge couplers can only be placed near the chip facets. This requires careful chip preparation and it does not allow testing of fabricated devices on a wafer scale. Surface grating couplers are an alternative approach for coupling of light to or from microphotonic waveguide circuits. These grating couplers can be placed at specific locations on the chip, thus enabling wafer-scale testing [2]. To achieve high coupling efficiency, the grating must have a high directionality (defined as the fraction of power diffracted upwards) towards the fiber situated above the chip and the radiated field should match the near-Gaussian field of the optical fiber mode. Grating directionality is significantly affected by the interference condition from the substrate layers, specifically with a strong dependence on buried oxide (BOX) thickness [6]. Grating directionality can be improved using thicker silicon waveguides [7, 8], instead of a typical thickness of 220 nm that is often used in silicon photonic foundries. Specialized grating structures [6–10] can provide high directionalities, but at the expense of increased fabrication complexity. The coupling efficiency can be further optimized by controlling the grating strength. Different approaches have been demonstrated, based on single etch steps [7] or multiple etch steps [8, 10] in combination with duty cycle optimization. Recently, utilization of subwavelength structured materials [11] was shown to afford a marked flexibility in grating coupler design [12, 13], including broadband [14], polarization-independent [15], and mid-infrared [16] structures.

[1] University of Žilina, Faculty of Electrical Engineering, Department of Telecommunication and Multimedia, Univerzitná 8215/1, 010 26 Žilina, Slovakia
[2] National Research Council Canada, Building M50, 1200 Montreal Road, Ottawa, Ontario, Canada K1A 0R6
[3] Departamento de Ingeniería de Comunicaciones, ETSI Telecomunicación, Universidad de Málaga, 29010 Málaga, Spain
*Corresponding authors: e-mail: daniel.benedikovic@fel.uniza.sk, pavel.cheben@nrc-cnrc.gc.ca

In this work, a detailed design procedure and experimental demonstration of a high-efficiency SWG coupler are presented. We show that, by judicious adjustment of the radiation angle, the coupling efficiency can be maximized for arbitrary BOX thickness. The grating is apodized by SWG refractive index engineering [12], which allows fabrication with a single etch step. We also demonstrate using simulations how this approach can be directly applied for designing highly efficient grating couplers in established CMOS-compatible fabrication processes.

Our SWG coupler is implemented in SOI waveguides with a silicon layer thickness of 220 nm, a BOX layer thickness of 3 μm, and air as a superstrate medium. The coupler is optimized for transverse electric polarization at a wavelength of 1550 nm using a tool based on the Fourier-eigenmode expansion method (F-EEM) [19] and verified using a two-dimensional finite difference time domain (FDTD) simulator [20].

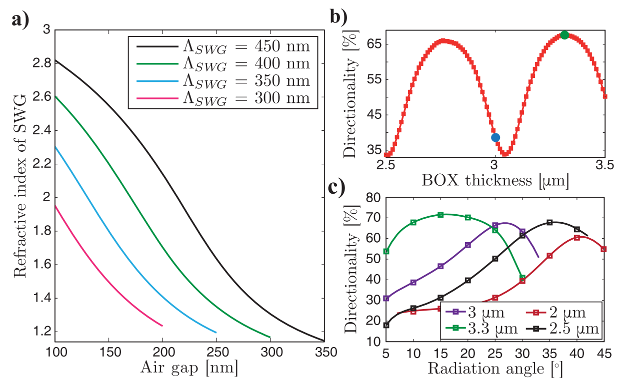

Figure 2 (a) Equivalent refractive index of SWG structure as a function of the air gap for various SWG periods. (b) Grating directionality as a function of BOX thickness for a radiation angle of 10°. (c) Grating directionality as a function of radiation angle for various BOX thicknesses.

2. Uniform grating coupler design

Instead of adjusting the shallow etch depth of grating grooves to engineer the grating strength [6–10], we use a fully etched SWG structure as was first proposed by Halir et al. [12], allowing efficient grating apodization and simplifying the fabrication. Decoupled two-dimensional models, illustrated in Fig. 1a and 1b, are used in the yz-plane and xz-plane to model the diffractive grating and the SWG structure.

The SWG is a periodic structure implemented by interleaving two constituent materials, here silicon and air, with refractive indices $n_{\mathrm{Si}} = 3.476$ and $n_{\mathrm{air}} = 1$. The SWG periodicity is small enough to suppress diffraction so that the structure acts as a homogeneous medium with equivalent refractive index [11], here denoted as n_{SWG}. This index is calculated by considering the SWG structure as a multilayer slab waveguide [12]. The effective refractive index of the slab waveguide fundamental mode is tuned by varying the SWG duty cycle, defined as $\mathrm{DC}_{\mathrm{SWG}} = (1 - G/\Lambda_{\mathrm{SWG}})$, where G is the size of the air gap and Λ_{SWG} is the SWG period. As shown in Fig. 2a, a broad range of refractive indices can be realized depending on the minimum feature size of the fabrication process.

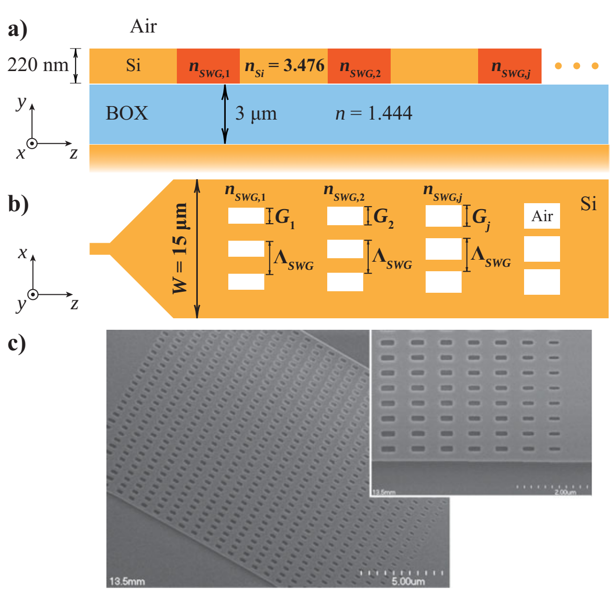

Figure 1 (a) Two-dimensional vertical cross-section schematic of SWG coupler. (b) Two-dimensional in-plane schematic of SWG coupler. (c) Scanning electron microscopy image of fabricated continuously apodized coupler. Inset: detailed view.

As a reference structure, we designed a uniform grating coupler by alternating lines of unpatterned silicon and the artificial medium to adjust the grating strength. According to our calculations, the SWG index $n_{\mathrm{SWG}} = 2.40$ yields the maximum near-field overlap with the SMF-28 optical fiber mode. This index is achieved for gap $G = 171$ nm and SWG period $\Lambda_{\mathrm{SWG}} = 450$ nm, which is sufficiently small to suppress diffraction. The grating consists of 25 periods, each of length $\Lambda_z = 718$ nm and duty cycle $\mathrm{DC}_z = 55\%$, yielding a radiation angle in air of 10°. The grating radiates 39% of power into the superstrate. The SWG structure effectively reduces the grating strength and an overlap of up to 74% is achieved. The calculated back reflection is 7.3%. The coupling loss of uniform coupler is -5.3 dB.

An important drawback of this structure is a limited directionality due to the destructive interference with the field reflected at the interface between BOX and silicon substrate, yielding 51% of power radiated down to the substrate. Figure 2b shows the periodical dependence of the grating directionality as a function of the BOX thickness, with maxima near 2.7 μm and 3.3 μm. However, SOI wafers have a standard BOX thickness (2 and 3 μm) and freedom of choosing a different BOX thickness is limited. Here we propose to overcome this limitation by modifying the grating radiation angle. By judicious adjustment of the radiation angle, constructive interference can be achieved for a given BOX thickness. The directionality can be significantly increased, as shown in Fig. 2c. The grating is redesigned to operate with a radiation angle of 27° for diffraction period $\Lambda_z = 810$ nm and duty cycle $\mathrm{DC}_z = 55\%$. The calculated SWG index is $n_{\mathrm{SWG}} = 2.40$ and the gap size is $G = 171$ nm. This design shows an increased upward radiated power of 68%, while the power radiated downwards is reduced to 28%. The mode field overlap is increased to 78% and the back reflections are reduced to 2.4%. The calculated coupling loss is −2.56 dB with a 3 dB bandwidth of 60 nm, i.e. the coupling loss is nearly doubled compared to the design with a nominal radiation angle of 10°. Our F-EEM simulation results are in good agreement with FDTD calculations.

3. Apodized grating coupler design

The SWG structure enables grating apodization, which overcomes the theoretical overlap limit of ∼80%. To control the grating contrast along the propagation direction, variable SWG indices are realized to produce a gradual modification of coupling strength. For the apodized design, the phase of the diffracted field has to be constant for all periods to ensure the same radiation angle of 27° according to the phase matching condition: $k\lambda = \Lambda_{z,j}(n_{\mathrm{B},j} - \sin\Theta_j)$, where λ is the wavelength, k is the diffraction order, $\Lambda_{z,j}$ is the grating period, and $n_{\mathrm{B},j}$ is the effective index of Bloch mode for jth grating period. To fulfill the phase matching condition for the grating trenches of variable SWG index, the diffraction periods are correspondingly chirped.

We designed a two-step apodized grating coupler with two sections of different SWG indices. As a result, we found that the near-field overlap is increased to 88% and back reflection is reduced to 1%. The two-step grating coupler consists of 22 periods, specifically of 4 periods with pitch $\Lambda_{z,1} = 760$ nm and a higher SWG index $n_{\mathrm{SWG},1} = 2.70$, followed by 18 periods with pitch $\Lambda_{z,2} = 810$ nm and a lower index $n_{\mathrm{SWG},2} = 2.40$. A duty cycle $\mathrm{DC}_z = 55\%$ is used for both sections. The lateral air gaps $G_1 = 124$ nm and $G_2 = 171$ nm are within the range of deep-ultraviolet (DUV) lithography. The calculated coupling loss of the two-step apodized grating coupler is −2.2 dB with a 3 dB bandwidth of 62 nm.

Further improvement is achieved by a continuous apodization of the grating. A linear variation of SWG trench index from 2.80 to 2.20 along the first 10 grating periods is used with $\Lambda_{\mathrm{SWG}} = 450$ nm and a feature size of about 100 nm. The lateral gaps are varied from 104 to 194 nm and the diffraction periods are adjusted from 751 to 847 nm with a duty cycle $\mathrm{DC}_z = 55\%$. The second part of the grating has trenches with SWG index of 2.20 along 15 periods of pitch $\Lambda_z = 847$ nm. The continuously apodized grating has a directionality of 69% and the field overlap is improved to 92%. The calculated coupling loss is −1.97 dB with a 3 dB bandwidth of 66 nm, which is in good agreement with FDTD simulations. The back reflection is 3.5%, which is higher than that of the two-step apodized design. This can be solved by increasing the SWG index at the interface of the injection waveguide at the expense of a smaller feature size (<100 nm) or by curving and offsetting the grating lines [21].

4. Grating coupler fabrication and experimental results

To experimentally demonstrate the validity of our design method, grating couplers were fabricated on a standard SOI wafer with Si layer thickness of 220 nm and BOX layer thickness of 3-μm. The grating couplers and interconnecting waveguides were defined in a single step using electron beam lithography. The resist pattern was fully etched using inductively coupled plasma reactive ion etching. A scanning electron microscopy (SEM) image of a fabricated continuously apodized coupler is shown in Fig. 1c. With rectangular air holes used in the layout, some corner rounding can be observed due to fabrication resolution limit. The influence of this effect on coupler performance was shown to be minimal, even for comparatively large shape distortions (elliptical holes) in SWG structures fabricated using 193 nm DUV lithography [17, 18].

To facilitate optical characterization, grating couplers were arranged in a back-to-back configuration, with input and output polarization-maintaining optical fibers polished at an angle. In this arrangement, the fiber facets are oriented parallel to the chip surface, refracting light at the fiber–air interface at the required coupling angle. This technique can be customized for a specific coupling angle and extended to fiber arrays [22]. The coupling loss was determined from the measured insertion loss of two back-to-back connected couplers, subtracting the loss of the silicon wire interconnecting waveguide. The experimental results for the two-step apodized and the continuously apodized grating couplers are shown in Fig. 3. A measured peak coupling loss for the two-step apodized grating is −2.98 dB at a wavelength of 1531 nm with a 3 dB bandwidth of 61 nm. Compared to the simulation results, the experimental coupling loss is 0.78 dB higher with a noticeable blue shift (∼20 nm) in the central wavelength. The performed SEM measurements show lateral gap dimensions $G_1 = 109$ nm and $G_2 = 154$ nm and longitudinal duty cycle $\mathrm{DC}_{z,1} = 59\%$ and $\mathrm{DC}_{z,2} = 56\%$, slightly different from the nominal values. We simulated grating performance with the actual dimensions measured using SEM, yielding a coupling loss of −3.1 dB, which

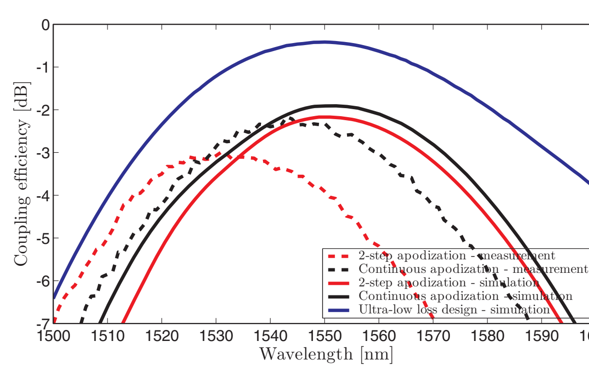

Figure 3 Simulated and measured coupling efficiency as a function of wavelength for the two-step apodized, the continuously apodized, and the sub-decibel SWG fiber–chip couplers.

is in good agreement with experimental results. The measured coupling loss of the continuously apodized coupler is −2.16 dB at a wavelength of 1543 nm with a 3 dB bandwidth of 64 nm. This is one of the lowest losses yet reported for single etch step grating couplers. The measured results are comparable to those achieved for apodized shallow etched grating couplers that, however, require thicker non-standard silicon waveguides [7, 8, 23], small feature size (50 nm) [7, 10], or additional etch steps and increased fabrication complexity [6–10]. A good agreement with simulations is observed, with a loss penalty of less than 0.2 dB and small blue shift (∼5 nm) in the central wavelength. This is corroborated by SEM inspection (inset of Fig. 1c), confirming that the fabricated parameters are close to the nominal design dimensions. In addition, simulations show that average dimension variations along the grating coupler are ∼8 nm with a coupling loss of −2.18 dB, which is in excellent agreement with experimental results.

5. Sub-decibel grating coupler design

Grating apodization by SWG engineering is an efficient method for increasing the overlap between the diffracted field and the optical fiber mode. However, the remaining obstacle to further increasing the coupling efficiency is the loss penalty due to the power radiated to the substrate. Here we propose to utilize a double-SOI wafer, which enables standard silicon photonic fabrication [24, 25]. We implement our grating design in this modified SOI platform formed by alternating two high-refractive-index (Si) layers and two low-refractive-index (SiO_2) layers, each of optical thickness of $\lambda/4$, on the silicon substrate. The grating consists of 15 apodized periods with linearly varied SWG indices from 2.80 to 2.30, with feature size of 100 nm for $\Lambda_{SWG} = 450$ nm. According to our calculations, the grating coupler exhibits an excellent directionality of 98%. The SWG apodization yields a high overlap of 92.8% and back reflections are reduced to 0.6%. The overall coupling loss of this design is −0.42 dB, which is in excellent agreement with FDTD simulations. This arguably is one of the highest calculated coupling efficiencies hitherto reported for a fiber–chip surface grating coupler in SOI. Alternatively, backside processing with metal deposition below the BOX layer implemented in a standard SOI wafer is the state-of-the-art technique for high-efficiency grating couplers [10]. Our FDTD calculations for a grating coupler with backside metal deposition predict an improved directionality of 93%. Both presented approaches yield significant improvement in calculated grating directionality, with promising prospects towards development of sub-decibel-efficiency fiber–chip grating couplers.

6. Conclusion

We designed and fabricated SWG-based apodized fiber-to-chip grating couplers. Using SWG engineering, devices can be fabricated in a single etch step. In particular, we demonstrated that diffraction angle adjustment can be used to design high-efficiency single etch grating couplers on a standard SOI platform. A peak coupling efficiency of −2.16 dB was measured and our calculations show a high efficiency of −0.42 dB using a modified SOI structure with a bottom reflector that further improves the coupler directionality. These results offer a good perspective for the design of low-cost grating couplers in high volume using 193 nm DUV lithography compatible with mass fabrication.

Acknowledgement. This work was supported by the Slovak Research and Development Agency (APVV-0025-12), Slovak Grant Agency (VEGA 1/1271/12) and National Research Council Canada.

Received: 28 April 2014, **Revised:** 8 August 2014,
Accepted: 8 September 2014

Published online: 15 October 2014

Key words: Integrated optics, fiber–chip grating coupler, silicon-on-insulator (SOI), subwavelength grating (SWG).

References

[1] T. Tsuchizawa, K. Yamada, H. Fukuda, T. Watanabe, J. Takahashi, M. Takahashi, T. Shoji, E. Tamechika, S. Itabashi, and H. Morita, IEEE J. Sel. Top. Quant. Electron. **11**, 232–240 (2005).
[2] A. Mekis, S. Gloeckner, G. Masini, A. Narasimha, T. Pinguet, S. Sahni, and P. De Dobbelaere, IEEE J. Sel. Top. Quant. Electron. **17**, 597–608 (2011).
[3] V. Almeida, R. Panepucci, and M. Lipson, Opt. Lett. **28**, 1302–1304 (2003).
[4] P. Cheben, P. J. Bock, J. H. Schmid, J. Lapointe, S. Janz, D. Xu, A. Densmore, A. Delage, B. Lamontagne, and T. J. Hall, Opt. Lett. **35**, 2526–2528 (2010).
[5] R. Takei, M. Suzuki, E. Omoda, S. Manako, T. Kamei, M. Mori, and Y. Sakakibara, Appl. Phys. Lett. **102**, 101–108 (2013).
[6] F. Van Laere, G. Roelkens, M. Ayre, J. Schrauwen, D. Taillaert, D. Van Thourhout, T. F. Krauss, and R. Baets, J. Lightwave Technol. **25**, 151–156 (2007).
[7] X. Chen, C. Li, K. Y. Fung, S. M. G. Lo, and H. K. Tsang, IEEE Photon. Technol. Lett. **22**, 1156–1158 (2010).
[8] Ch. Li, H. Zhang, M. Yu, and G. Q. Lo, Opt. Express **21**, 7868–7874 (2013).
[9] D. Vermeulen, S. Selvaraja, P. Verheyen, G. Lepage, W. Bogaerts, P. Absil, D. Van Thourhout, and G. Roelkens, Opt. Express **18**, 18278–18283 (2010).
[10] W. S. Zaoui, A. Kunze, W. Vogel, M. Berroth, J. Butschke, F. Letzkus, and J. Burghartz, Opt. Express **22**, 1277–1286 (2014).
[11] S. M. Rytov, Sov. Phys. JETP **2**, 466–475 (1956).
[12] R. Halir, P. Cheben, J. H. Schmid, R. Ma, D. Bedard, S. Janz, D.-X. Xu, A. Densmore, J. Lapointe, and I. Molina-Fernández, Opt. Lett. **35**, 3243–3245 (2010).
[13] Y. Ding, H. Ou, and Ch. Peucheret, Opt. Lett. **38**, 2732–2734 (2013).

[14] X. Chen, K. Xu, Z. Cheng, C. K. Fung, and H. K. Tsang, Opt. Lett. **37**, 3483–3485 (2012).
[15] X. Chen and H. K. Tsang, Opt. Lett. **36**, 796–798 (2011).
[16] Z. Cheng, X. Chen, C. Y. Wong, K. Xu, and H. K. Tsang, Opt. Lett. **37**, 5181–5183 (2012).
[17] R. Halir, L. Zavargo-Peche, D.-X. Xu, P. Cheben, R. Ma, J. H. Schmid, S. Janz, A. Densmore, A. Ortega-Moñux, I. Molina-Fernández, M. Fournier, and J.-M. Fédeli, Opt. Quant. Electron. **44**, 521–526 (2012).
[18] R. Halir, I. Molina-Fernandez, P. Cheben, J. H. Schmid, R. Ma, S. Janz, D. Xu, A. Densmore, and J. Fedeli, in: Proceedings of the ICO International Conference on Information Photonics, Ottawa, ON, Canada, 18–20 May 2011, pp. 1–2.
[19] L. Zavargo-Peche, A. Ortega-Moñux, J. G. Wangüemert-Pérez, and I. Molina-Fernández, Prog. Electromagn. Res. **123**, 447–465 (2012).
[20] Optiwave [Online]. Available: www.optiwave.com.
[21] Y. Li, D. Vermeulen, Y. De Koninck, G. Yurtsever, G. Roelkens, and R. Baets, Opt. Lett. **37**, 4356–4358 (2012).
[22] B. Snyder and P. O'Brien, IEEE Trans. Compon. Packag. Manuf. Technol. **3**, 954–959 (2013).
[23] D.-X. Xu, J. H. Schmid, G. T. Reed, G. Z. Mashanovich, D. J. Thomson, M. Nedeljkovic, X. Chen, D. Van Thourhout, S. Keyvaninia, and S. K. Selvaraja, IEEE J. Sel. Top. Quant. Electron. **20**, 189–205 (2014).
[24] M. K. Emsley, O. Dosunmu, and M. S. Ünlü, IEEE J. Sel. Top. Quant. Electron. **8**, 948–955 (2002).
[25] F. Boeuf et al., in: Proceedings of the IEEE International Electron Devices Meeting (IEDM), Washington, DC, USA, 9–11 December 2013, pp. 13.3.1–13.3.4.